Reactive ion etching of Ta–Si–N diffusion barriers in CF_4+O_2

G. F. McLane and L. Casas
Army Research Laboratory, Ft. Monmouth, New Jersey 07703

J. S. Reid, E. Kolawa, and M.-A. Nicolet
California Institute of Technology, Pasadena, California 91125

(Received 22 February 1994; accepted 24 May 1994)

$Ta_{36}Si_{14}N_{50}$ amorphous layers were reactive ion etched in CF_4+O_2 plasmas. The etch depth was determined as a function of gas composition, pressure, and cathode power. Adding small amounts of O_2 to CF_4 increased the etch rates up to approximately 15% O_2 concentration, with etch rates then decreasing with further addition of O_2. Etch rates increased with both pressure and power. Etching proceeded only after an initial delay time which depended upon gas composition and power. The delay is probably caused by a surface native oxide which must be removed before etching can commence. The presence of a surface oxide was observed from Auger electron spectroscopy intensity depth profile measurements and is estimated to be 2 nm thick. Under optimal conditions, the etch rate of $Ta_{36}Si_{14}N_{50}$ is about seven times higher than for SiO_2, thus providing a high degree of selectivity for integrated circuit processing.

I. INTRODUCTION

Ta–Si–N is an amorphous conducting alloy with a high crystallization temperature and strong chemical stability. This material has been shown to be an exceptional diffusion barrier in silicon metallizations[1–4] as well as an excellent encapsulant for III–V semiconductors.[3,5,6] As a requisite for incorporation into high-density integrated circuit processing, Ta–Si–N must be patternable into small structures, preferably by dry etching. Plasma etching of both $TaSi_2$ (Ref. 7) and Si_3N_4 (Refs. 8–10) in CF_4+O_2 mixtures has been previously demonstrated. We report here results obtained on reactive ion etching (RIE) of $Ta_{36}Si_{14}N_{50}$ amorphous buffer layers in similar CF_4+O_2 mixtures.

II. EXPERIMENT

Thin films of $Ta_{36}Si_{14}N_{50}$ were deposited onto (100) Si substrates by rf sputtering of a Ta_5Si_3 target in an Ar/N_2 discharge as detailed elsewhere.[1] Etching of 150 nm thick films in CF_4+O_2 was performed in a Plasmalab μ Etch RIE system with a 24 cm diameter water-cooled cathode driven by a 13.56 MHz power supply. The film samples were patterned with AZ5214 photoresist, and etch depths were determined from Dektak profilometer measurements. Gas mixture composition was adjusted by varying the amount of gas flow through the CF_4 and O_2 flow meters. For comparative purposes, the etch rates of thermally grown SiO_2 were also measured under similar conditions. SiO_2 is a common passivation material in integrated circuits, and thus a high degree of selectivity in etching Ta–Si–N over SiO_2 is desirable. Auger electron spectroscopy (AES) intensity depth profiles were measured in a Perkin Elmer PHI 660 scanning Auger microprobe using a 10 kV electron beam with a 4 kV Ar^+-ion beam for sputtering.

An etch rate dependence on chamber condition and history is sometimes observed with a CF_4+O_2 plasma.[11] This dependence can be attributed to the presence of a polymer coating on the chamber walls which can affect plasma chemistry. For our experiments, this effect was more evident at the lower O_2/CF_4 ratios, and several etch runs sometimes had to be performed for a given set of etching parameters in order to "condition" the chamber and obtain reproducible results.

III. RESULTS AND DISCUSSION

Fluorine atoms are created in a CF_4 plasma and produce volatile SiF_4 (Ref. 8) and Ta-fluoride (Ref. 12) etch products. When oxygen is added to a CF_4 plasma, it reacts with carbon species to form molecules such as CO_2, CO, and COF_2, limiting the recombination of F atoms and freeing them for the etching process. The net result is an increase in etch rate as O_2 is added to CF_4. However, sufficiently high O_2 concentrations will ultimately reduce the etch rate due to a dilution effect, and therefore, an O_2 concentration can usually be found which will produce the maximum etch rate.

Figure 1 shows $Ta_{36}Si_{14}N_{50}$ and SiO_2 etch depths as a function of O_2 concentration in a CF_4+O_2 plasma for a 1 min etch duration and fixed pressure and cathode power. The etch depth of $Ta_{36}Si_{14}N_{50}$ is a maximum at approximately 15% O_2 concentration. Harshbarger *et al.*[13] measured the optical emission intensity from atomic F as a function of O_2 concentration in a CF_4+O_2 plasma and reported a similar dependency with a maximum intensity at about the same 15% O_2 concentration. The results of Fig. 1 indicate the expected correlation between the Ta–Si–N etch rate and F atom concentration. Sun *et al.*[7] reported a similar reactive ion etch rate curve for amorphous sputtered $TaSi_2$ etched in CF_4+O_2, which had a maximum etch rate for 4% O_2 concentration. Figure 1 also shows that the etching of SiO_2 exhibits little dependence on gas composition, with lower etch rates than Ta–Si–N. Consequently, the CF_4+O_2 mixture satisfies selectivity requirements for many integrated circuit processes.

Since Ta-silicide etches more slowly than Si in fluorine-based discharges,[14] it is reasonable to assume that etching of Ta is the rate limiting process for Ta–Si–N materials. Indeed, TaF_5 has a much lower vapor pressure than SiF_4.[14] It has been reported[7] that reactive ion etching of $TaSi_2$ in

 0734-211X/94/12(4)/2352/4/$1.00 ©1994 American Vacuum Society

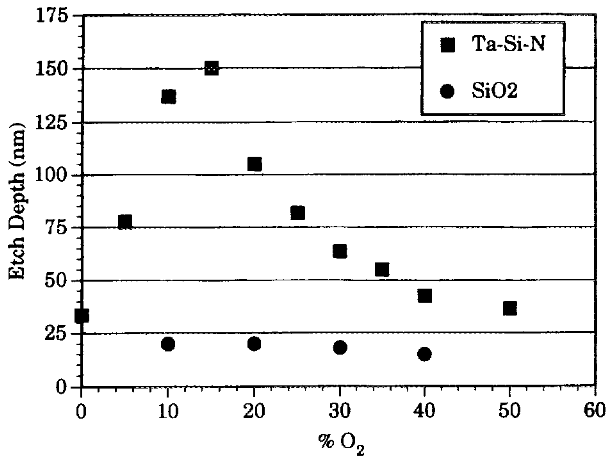

FIG. 1. $Ta_{36}Si_{14}N_{50}$ and SiO_2 etch depths as a function of percent of oxygen in CF_4+O_2 mixtures for 90 W power, 150 mTorr pressure, 40 sccm total flow rate, and 1 min etch time.

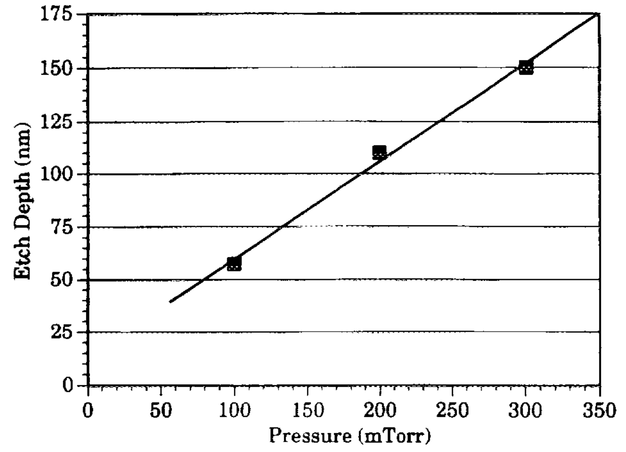

FIG. 3. $Ta_{36}Si_{14}N_{50}$ etch depth as a function of pressure for 50 sccm flow rate consisting of $25O_2/25CF_4$ sccm flow rate mixture, 90 W power, and 2 min etch time.

CF_4+O_2 plasmas results in the etched surface becoming Ta rich. However, AES depth profile measurements of an etched Ta–Si–N layer reveal no such Ta-rich surface in our case.

The dependence of etch depth on cathode power is exhibited in Fig. 2. As power increases, the plasma density and associated concentration of reactive species (F atoms) should also increase, producing higher etch rates and resultant etch depths for a given etch time. Figure 3 shows that the etch depth also increases with chamber pressure. As pressure is increased, the density of CF_4+O_2 and the resultant F atom concentration also increase, again producing higher etch rates. The power and pressure dependence of the etch depth indicates that the etch rate is limited by F atom production under the given conditions. Figure 4 shows a scanning electron micrograph of a Ta–Si–N sample patterned with AZ5214 photoresist and etched in CF_4+O_2. The etched surface is smooth and the sidewalls are sloped due to erosion of the mask edge.

The dependence of etch depth on etching time for several concentrations of O_2 in a CF_4+O_2 plasma is shown in Fig.5. Etching proceeds only after an initial delay time which depends upon etch gas composition. This delay time varies from about 0.6 min for 40%–50% O_2 concentration, down to about 0.3 min for 15% O_2 concentration. Figure 6 shows the dependence of etch depth on time for several values of cathode power. Again, a delay in the onset of etching is observed, with the amount of the time delay decreasing as cathode power increased. We speculate that this delay is caused by the presence of a surface oxide which must be removed before etching of the Ta–Si–N can commence. Similar delays have been observed in the etching of GaAs[15,16] and AlGaAs[15–18] and have been attributed to the need to etch or sputter away the surface oxide. Since the time delay decreases as power increases and O_2 concentration decreases, it seems reasonable to assume that the presence of a surface

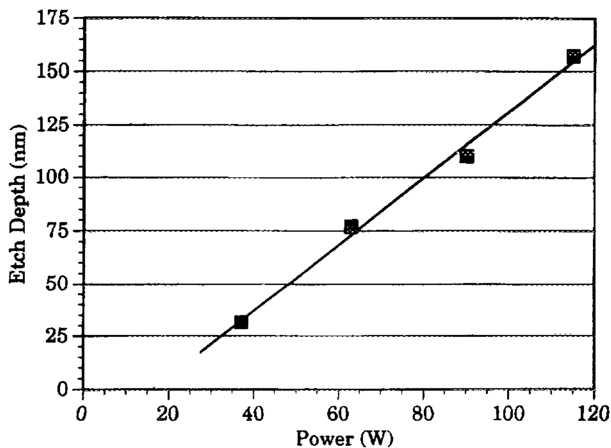

FIG. 2. $Ta_{36}Si_{14}N_{50}$ etch depth as a function of power for 50 sccm total flow rate consisting of $25O_2/25CF_4$ sccm flow rate mixture, 200 mTorr pressure, and 2 min etch time.

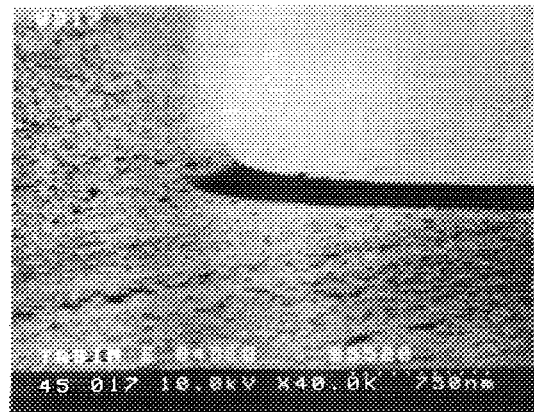

FIG. 4. Scanning electron micrograph of $Ta_{36}Si_{14}N_{50}$ sample patterned with AZ5214 photoresist mask. Etching parameters are 50 sccm total flow rate consisting of $25O_2/25CF_4$ sccm flow rate mixture, 63 W power, and 2 min etch time. Etch depth is 77 nm.

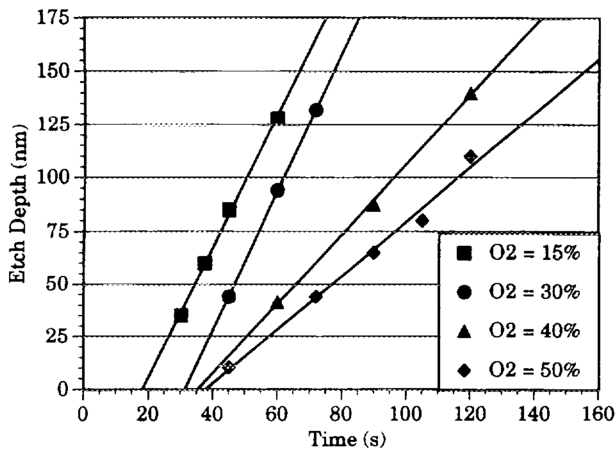

FIG. 5. $Ta_{36}Si_{14}N_{50}$ etch depth as a function of etch time for 90 W power, 200 mTorr pressure, and 50 sccm total flow rate consisting of 15%, 30%, 40%, and 50% oxygen in a CF_4+O_2 mixture.

oxide is responsible for the time delay; lower O_2 concentrations in the plasma result in less replenishment of the surface oxide during its removal, while higher powers cause faster removal of the surface oxide due to increased chemical etching and/or sputter etching.

The presence of a native oxide on the surface of an as-grown Ta-Si-N layer is seen from the data of Fig. 7, which shows an AES depth profile of Ta, Si, N, and O as a function of sputtering depth. Upon sputtering, the oxygen signal first increases and then decreases fairly quickly, indicating the presence of an oxide with an estimated thickness of 2 nm. Pokela *et al.*[19] have demonstrated the capability for growing much thicker oxides on $Ta_{36}Si_{14}N_{50}$ layers at 650–850 °C temperatures. In addition to the constituent Ta, Si, and N signals, small amounts of carbon and oxygen were detected in the Ta–Si–N layer, and were due to residues of these elements in the sputtering chamber. Since Ta has greater affinity for oxygen than does Si, the existence of a Ta oxide

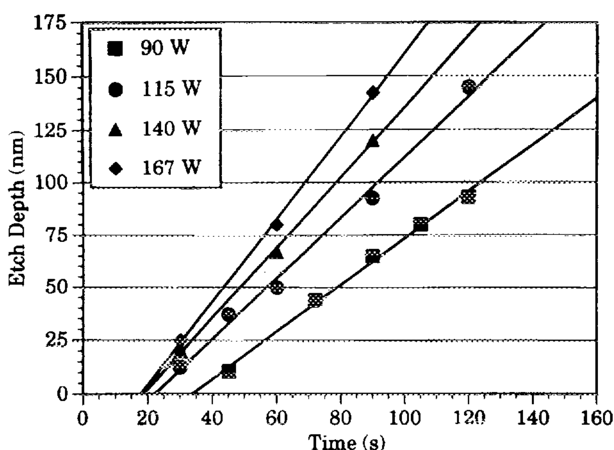

FIG. 6. $Ta_{36}Si_{14}N_{50}$ etch depth as a function of etch time for 200 mTorr pressure, 50 sccm total flow rate consisting of $25O_2/25CF_4$ sccm flow rate mixture, and 90, 115, 140, and 167 W power.

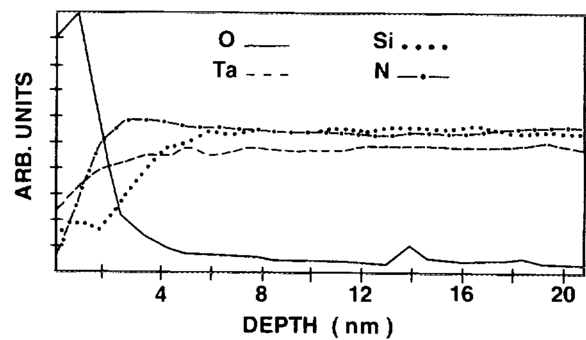

FIG. 7. Auger electron spectroscopy intensity depth profile of an as-grown $Ta_{36}Si_{14}N_{50}$ amorphous layer. Shown are the signals for tantalum, silicon, nitrogen, and oxygen as a function of Ar^+-ion sputtering depth.

could be the primary cause of this etching time delay. However, Sun *et al.*[7] found no delay in reactive ion etching of a sputtered amorphous $TaSi_2$ film in CF_4+O_2, for O_2 concentrations in the range 2%–12%. In any case, it appears that $Ta_{36}Si_{14}N_{50}$ has a fairly tenacious surface oxide.

Finally, it should be noted that the data of Figs. 1–3 are presented for a given total etch time, including the etching onset delay, and as such are not totally indicative of the dynamic rate of removal of Ta–Si–N material. However, correcting for the delay times will not affect the general etch rate dependencies which allow elucidation of the physical mechanisms underlying the etching process.

IV. SUMMARY

$Ta_{36}Si_{14}N_{50}$ sputtered amorphous layers have been reactive ion etched in CF_4+O_4 plasmas. The maximum etch rate is attained for approximately 15% O_2 concentration, with the etch rate mostly limited by F atom production. For this particular gas mixture, the selectivity of $Ta_{36}Si_{14}O_{50}$ over SiO_2 is about 7:1. Etching proceeds only after an initial delay time which varies depending upon gas composition and power. The delay time appears to be due to the presence of a native surface oxide which must first be removed before etching of the $Ta_{36}Si_{14}N_{50}$ can commence.

ACKNOWLEDGMENTS

The authors acknowledge A. Deanni for performing the sample patterning. Financial support for a portion of this work was provided by the Army Research Office.

[1]E. Kolawa, and M.-A. Nicolet, J. Vac. Sci. Technol. A **8**, 3006 (1990).
[2]E. Kolawa, P. J. Pokela, J. S. Reid, J. S. Chen, and M.-A. Nicolet, Appl. Surf. Sci. **53**, 373 (1991).
[3]E. Kolawa, J. S. Chen, J. S. Reid, P. J. Pokela, and M.-A. Nicolet, J. Appl. Phys. **70**, 1369 (1991).
[4]P. J. Pokela, E. Kolawa, M.-A. Nicolet, and R. P. Ruiz, J. Electrochem. Soc. **138**, 2125 (1991).
[5]J.M. Molarius, E. Kolawa, K. Morishita, M.-A. Nicolet, J. L. Tandon, J. A. Leavitt, and L. C. McIntyre, Jr., J. Electrochem. Soc. **138**, 834 (1991).
[6]J. S. Reid, R. P. Ruiz, E. Kolawa, J. S. Chen, J. Madok, and M.-A. Nicolet, Mater. Res. Soc. Symp. Proc. **260**, 555 (1992).
[7]S. P. Sun and S. P. Murarka, J. Electrochem. Soc. **135**, 2353 (1988).
[8]P. E. Riley and D. A. Hanson, J. Vac. Sci. Technol. B **7**, 1352 (1989).
[9]K. Jinno, Jpn. J. Appl. Phys. **17**, 1283 (1978).
[10]R. Kumar, C. Ladas, and G. Hudson, Solid State Technol. **19**, 54 (1976).

[11]T. Enomoto, M. Denda, A. Yasuoka, and H. Nakata, Jpn. J. Appl. Phys. **18**, 155 (1979).
[12]Y. Kuo, Jpn. J. Appl. Phys. **32**, 179 (1993).
[13]W. R. Harshbarger, R. A. Porter, T. A. Miller, and P. Norton, Appl. Spectrosc. **31**, 201 (1977).
[14]H. J. Mattausch, B. Hasler, and W. Beinvogl, J. Vac. Sci. Technol. B **1**, 15 (1983).
[15]K. Hikosaka, T. Mimura, and K. Joshin, Jpn. J. Appl. Phys. **20**, L847 (1981).
[16]R. Cheung, S. Thoms, M. Watt, M. A. Foad, C. M. Sotomayor-Torres, C. D. W. Wilkinson, U. J. Cox, R. A. Crowley, C. Dunscombe, and R. H. Williams, Semicond. Sci. Technol. **7**, 1189 (1992).
[17]S. J. Pearton, W. S. Hobson, and K. S. Jones, J. Appl. Phys. **66**, 5009 (1989).
[18]S. J. Pearton, W. S. Hobson, U. K. Chakrabarti, A. B. Emerson, E. Lane, and K. S. Jones, J. Appl. Phys. **66**, 2137 (1989).
[19]P. J. Pokela, J. S. Reid, C.-K. Kwok, E. Kolawa, and M.-A. Nicolet, J. Appl. Phys. **70**, 2828 (1991).